

Electronic Supplementary Information for:

Germanium-Silicon Alloy and Core-Shell Nanocrystals by Gas Phase Synthesis

*Christian Mehringer,^a Christian Kloner,^a Benjamin Butz,^b Benjamin Winter,^b Erdmann Spiecker,^b and
Wolfgang Peukert^{*a}*

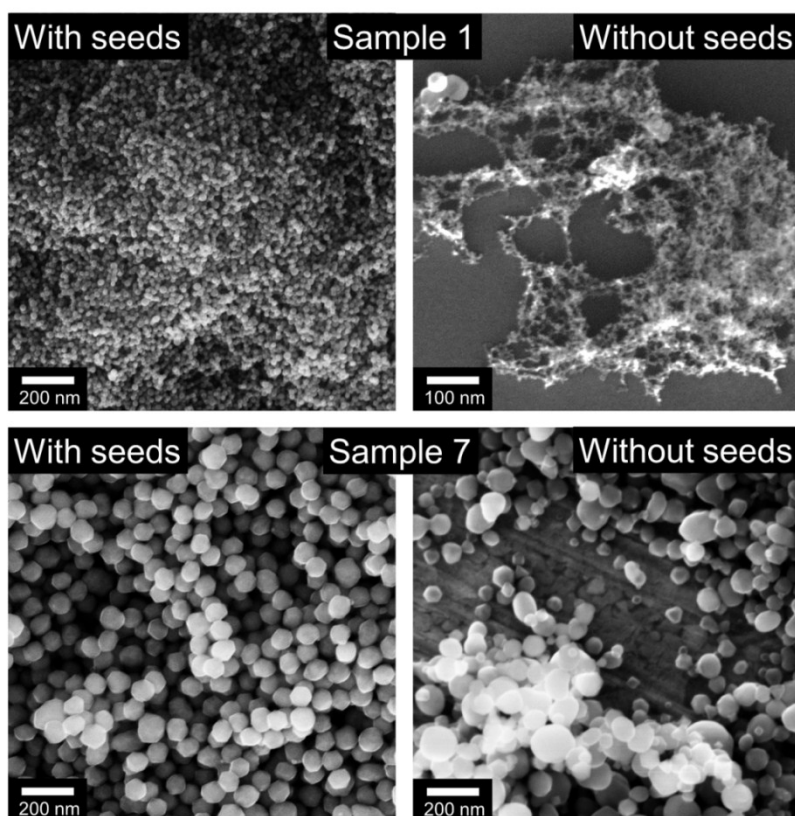
^a Institute of Particle Technology, Friedrich-Alexander-Universität Erlangen-Nürnberg

^b Center for Nanoanalysis and Electron Microscopy (CENEM), Friedrich-Alexander-Universität
Erlangen-Nürnberg

AUTHOR EMAIL ADDRESS: christian.mehringer@fau.de chris_kloner@gmx.de
benjamin.butz@ww.uni-erlangen.de benjamin.winter@ww.uni-erlangen.de
erdmann.spiecker@ww.uni-erlangen.de wolfgang.peukert@fau.de

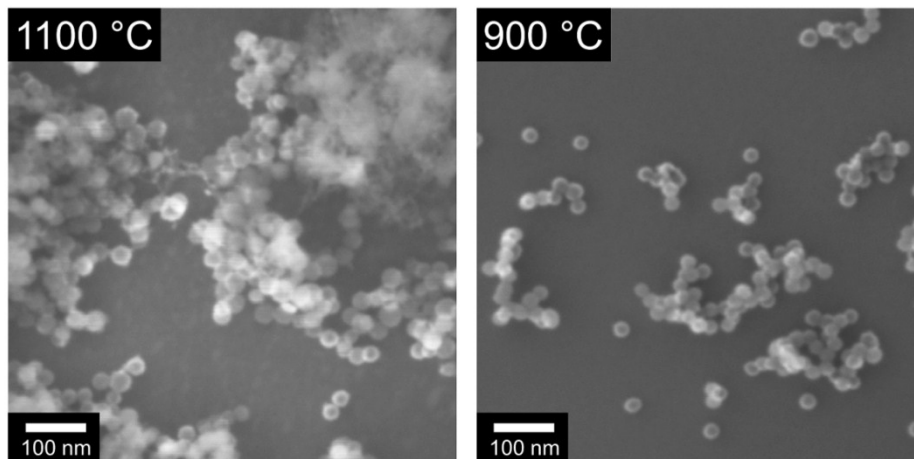
CORRESPONDING AUTHOR EMAIL ADDRESS: wolfgang.peukert@fau.de

Seeding



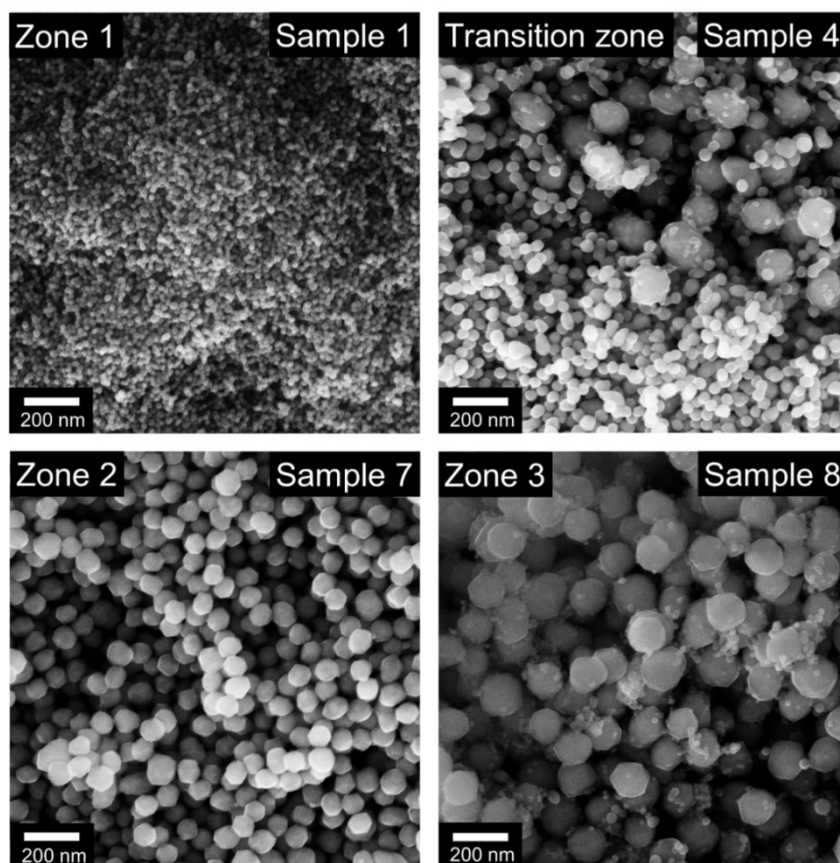
Suppl. Figure 1. SEM images of Samples 1 and 7 synthesized with and without seeding aerosol stream from HWR I.

The fact, that the seeding aerosol stream from HWR I is necessary becomes obvious in the SEM images depicted in Suppl. Figure 1. Samples 1 and 7 are prepared at exactly identical process conditions (also 900 °C temperature in HWR I), but no SiH₄ seeding volume flow. The very uniform morphology breaks down in both cases, proving that the seeds perform as heterogeneous nuclei for precursor deposition. In the case of the 25 mbar total pressure the seeds are smaller than 5 nm. XRD and gas sorption measurements performed on very small amounts of a prepared seed powder showed crystallite sizes of 1 nm and a primary particle size (Sauter diameter, BET method) of around 5 nm. No Si core was ever detected in the Ge-Si alloy particles. It is most likely dissolving in the evolving particle, with minor influence on the composition. At 75 mbar total pressure the seeding SiH₄ stream is forming different particles, as the Si inner cores of around 32 nm diameter in sample 7 show. However these are not the only species formed. Otherwise the morphology change would not be so drastic when we terminate the seeding. This becomes obvious when comparing impactor samples of the seeds synthesized at 75 mbar total pressure and 900 °C as well as 1100 °C synthesis temperature in HWR I, as shown in Suppl. Figure 2. At 900 °C only the particles that form the Si inner cores in the Ge-Si core-shell structures are visible. Increasing the temperature to 1100 °C leads to samples that also show very small particles arranged in cloud-like aggregates. The seeding at 75 mbar total pressure thus leads to an aerosol consisting of Si NPs around 32 nm in size and also very small particles. At 900 °C they neither show in our impactor samples, nor are they visible in the Ge-Si core shell particles without Si inner core. However, they strongly influence the product morphology, which is indirect prove that they also form at 900 °C.



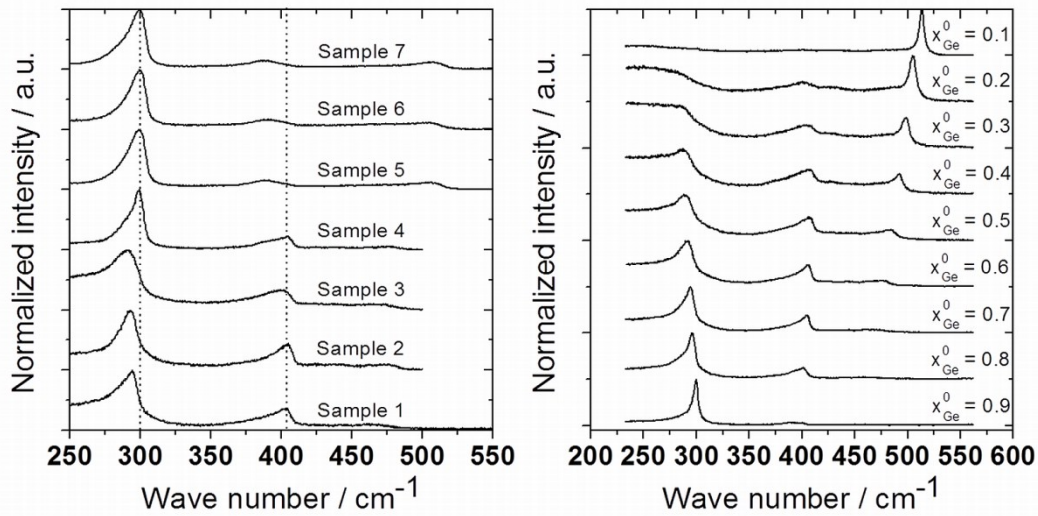
Suppl. Figure 2. SEM images of seeding particles synthesized at 75 mbar total pressure and 900 °C as well as 1100°C synthesis temperature in HWR I.

Morphology



Suppl. Figure 3. SEM images of representative particles from the zones in Figure 1. Zone 1 (Sample 1): $\sum p_{\text{Prec}} = 0.32$ mbar, $P_{\text{tot}} = 25$ mbar; Transition zone (Sample 4): $\sum p_{\text{Prec}} = 2.09$ mbar, $P_{\text{tot}} = 50$ mbar; Zone 2 (Sample 7): $\sum p_{\text{Prec}} = 4.04$ mbar, $P_{\text{tot}} = 75$ mbar; Zone 3 (Sample 8): $\sum p_{\text{Prec}} = 4.18$ mbar, $P_{\text{tot}} = 100$ mbar.

Raman analysis



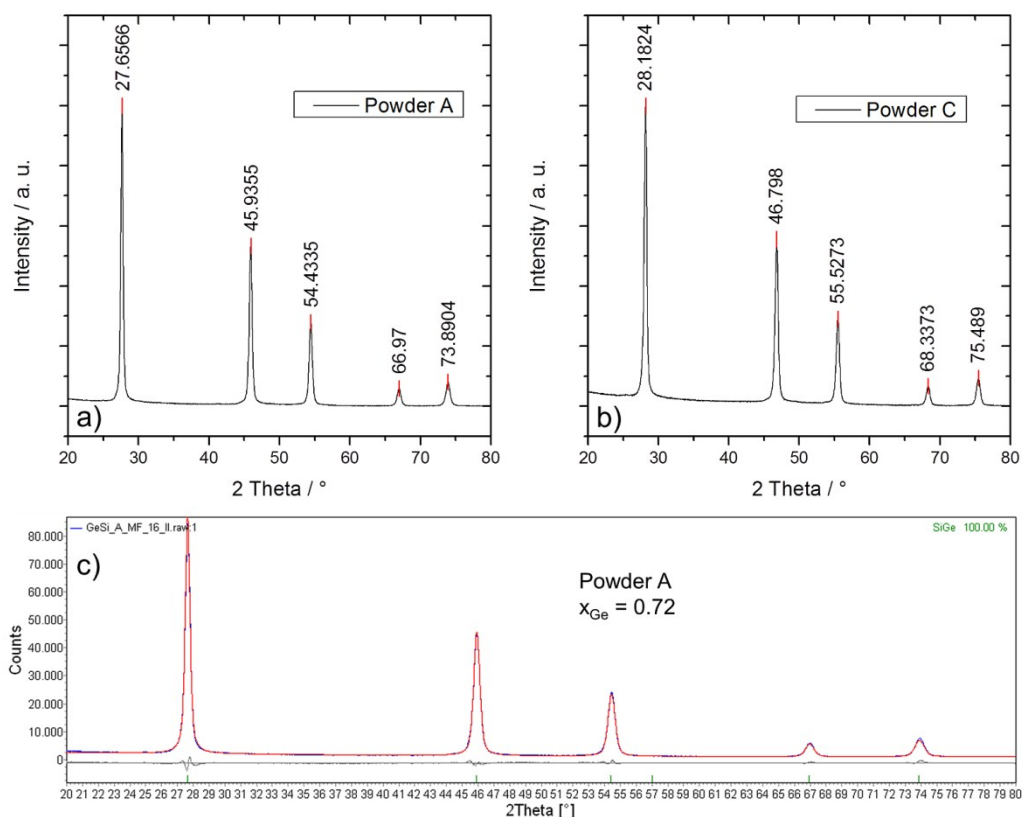
Suppl. Figure 4. Exemplary normalized Raman spectra of all samples utilized in the growth mode diagram determination. Samples 1 to 4 are only shown until 500 cm⁻¹, because the sample substrate was a Si wafer. The very intense Si peak from the substrate is left out. However the weak Si peak from the alloy sample is still observable.

Additional remarks on the Raman compositional analysis of alloy samples (Figure 3): A high Si content ($x_{Ge}^0 = 0.1$) leads to an intense Si-Si band at 514.4 ± 1 cm⁻¹, corresponding to an actual Ge content of $x_{Ge} = 0.09 \pm 0.01$. The alloy with equal Si and Ge content ($x_{Ge}^0 = 0.5$) clearly show all three peaks and the Si-Si band at 483.7 ± 0.6 cm⁻¹ indicating $x_{Ge} = 0.54 \pm 0.01$. The high Ge content alloy shows no Si-Si peak and a shift of the Ge-Ge band towards 300 cm⁻¹. In the case of $x_{Ge}^0 = 0.8$ this is 296.2 ± 0.3 cm⁻¹, corresponding to $x_{Ge} = 0.82 \pm 0.01$. The Ge content is increased in most samples as could be expected from the HWR II synthesis temperature variation shown in Figure 3a. According to Tsang *et al.*²³ for $x_{Ge} > 0.5$ the accuracy of the compositional analysis depends on the laser excitation wavelength and can be increased by using higher wavelengths than 532 nm. It is obvious, that the results obtained with 633 nm especially for $x_{Ge}^0 \leq 0.8$ are in good agreement with EDXS. This also proves that the alloy particles are fully relaxed because the Raman compositional analysis assumes zero strain. Taking these results as calibration, it is possible to deliver any desired composition by properly adapting the ratio of precursors in the feed. The resulting particles in all samples are of spherical shape and show a mean diameter of around 22 to 24 nm with a narrow size distribution as shown below (GSD of 1.14 to 1.19).

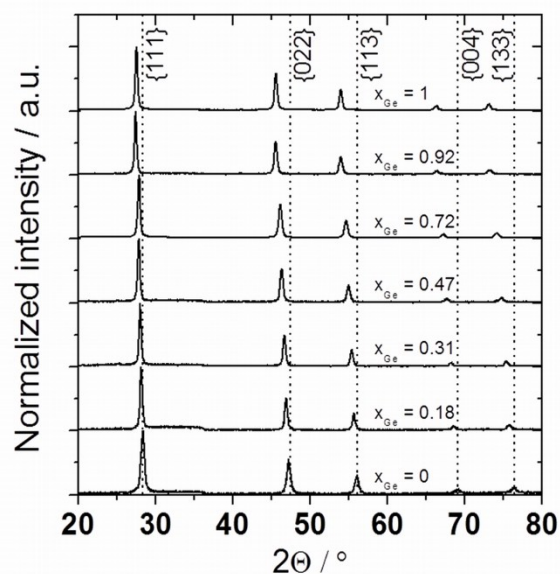
XRD Analysis

XRD is performed using a Bruker D8 Advance (Bragg-Brentano geometry) with CuK α -radiation (0.154 nm wavelength). The Bragg-angle (2θ) from 20° to 80° is covered in a step size of 0.021° with a measuring time of 2 s per step. Si single crystal containers (vicinal cut in [911]-direction) cased in PMMA sample holders are employed. The powder surface is pressed and prepared as flat as possible. The evaluation is done utilizing the software TOPAS (Bruker AXS) for peak fitting and simultaneous cell parameter refinement with a quantitative Rietveld analysis. In Suppl. Figure 5a+b the results for two alloy powder samples (synthesized in zone 1) are exemplarily depicted. Suppl. Figure 5c exemplarily shows how the original data (blue line) is fit with the diffractogram of an alloy with the (amongst others) calculated property x_{Ge} (red line). The grey line is the residual, which is very small in every case. The composition corresponds to the Raman and EDXS results (see Suppl. Table 1) and

together with the HRTEM proves that the samples are crystalline. No peak tailing or double peaks are observed which would indicate separation between Si and Ge. All diffractograms are shown in Suppl. Figure 6.



Suppl. Figure 5. a+b) Powder diffractograms of powder samples A and C containing peak position. c) Representative example of fitting. The measured data (blue lines) are fit (red lines) very well with Ge-Si alloys of a specified Ge content. The grey line represents the residual, which is very small in every data-set.

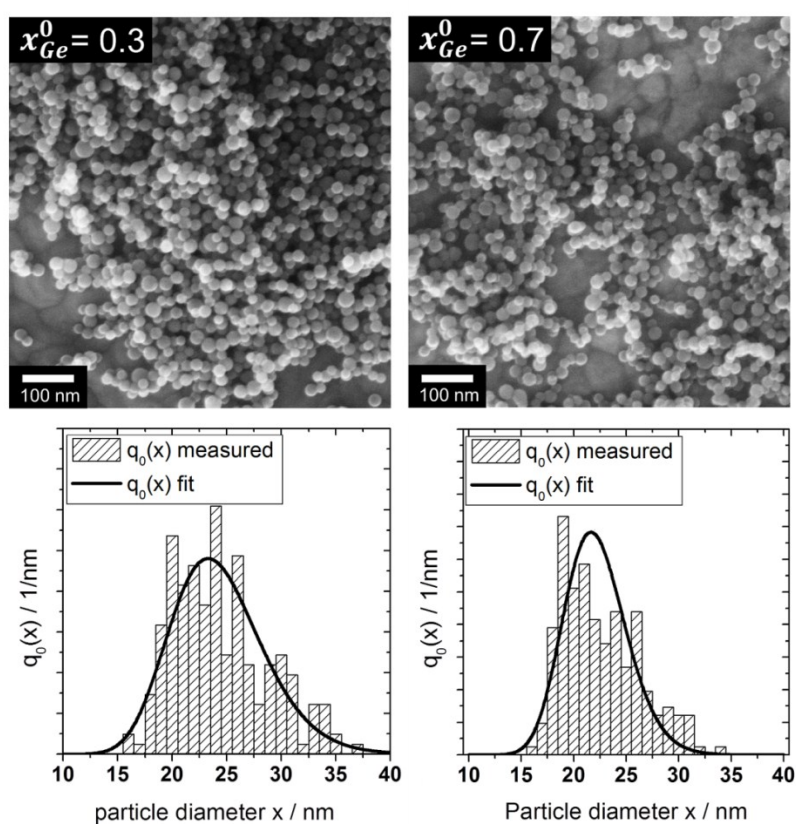


Suppl. Figure 6. Diffractograms of all powder samples.

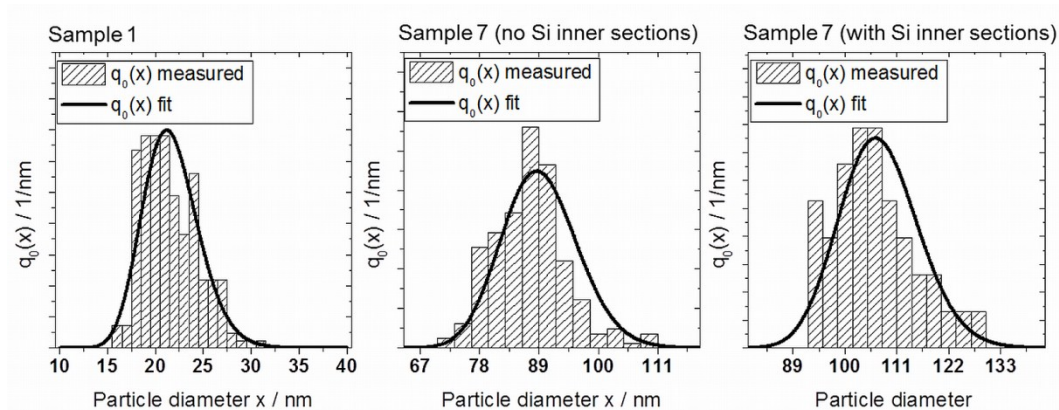
Suppl. Table 1. Comparison of EDXS, XRD and Raman compositional analysis performed on the Ge-Si alloy NCs.

	Nominal x_{Ge}^0	Actual x_{Ge}			
		Raman	XRD	EDXS Titan	EDXS SEM
Powder C	30	26	28	31.8	34
Powder B	50	48	47	45.7	54
Powder A	70	68	72	72.5	70

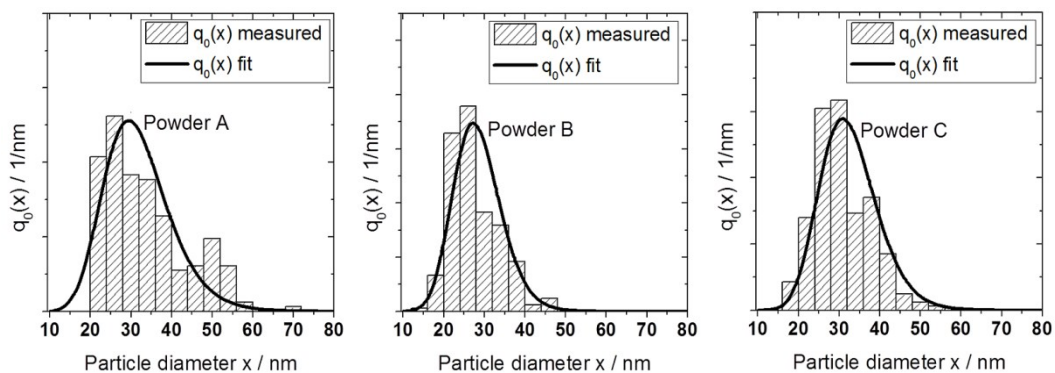
Particle Size Distributions (PSDs)



Suppl. Figure 7. SEM images and corresponding PSDs for alloy NC samples ($T_{HWRH} = 1000$ °C) with nominal compositions $x_{Ge}^0 = 0.3$ (24 nm, GSD = 1.19) and $x_{Ge}^0 = 0.7$ (22 nm, GSD = 1.14).



Suppl. Figure 8. PSDs for sample 1 (21.5 nm, GSD = 1.14), sample 7 with no Si inner sections (89 nm, GSD = 1.08) and sample 7 with Si inner sections (107 nm, GSD = 1.08).



Suppl. Figure 9. PSDs for powder samples A to C, determined from TEM images.